European Radiology (2019) 29:6447–6457
https://doi.org/10.1007/s00330-019-06258-w

GASTROINTESTINAL

Combination of CT findings can reliably predict radiolucent common bile duct stones: a novel approach using a CT-based nomogram

Ji Hye Min[1] · Kyung Sook Shin[2] · Jeong Eun Lee[2] · Seo-Youn Choi[3] · Soohyun Ahn[4]

Received: 13 January 2019 / Revised: 18 April 2019 / Accepted: 29 April 2019 / Published online: 21 May 2019

Abstract

Objectives To identify CT features that reliably predict the presence of radiolucent common bile duct (CBD) stones.

Materials and methods This retrospective study included 112 patients (mean age, 60.6 years) with clinically suspected CBD stones that were not visible on CT. All patients had undergone CT followed by endoscopic retrograde cholangiopancreatography (ERCP) to confirm the presence ($n = 66$) or absence ($n = 46$) of CBD stones. Two radiologists independently evaluated the CT images. Univariable and multivariable logistic regression analyses were performed to identify demographic, laboratory, and CT predictors for CBD stones. We developed a nomogram based on these results and assessed its performance.

Results In the multivariate analysis, CBD diameter ≥ 8 mm (odds ratio [OR], 10.12; $p < 0.001$), pericholecystic fat infiltration (OR, 3.76, $p = 0.014$), and papillitis (OR, 2.85; $p < 0.049$) were independent CT predictors of CBD stones. Combination of all three features had a specificity of 100%. Of these features, CBD diameter ≥ 8 mm was the best single predictor. The CT-based nomogram had an area under the curve (AUC) of 0.847 (95% confidence interval [CI], 0.777–0.916) and an accuracy of 77.7% (95% CI, 69.1–84.4%).

Conclusions The combination of significant CT features (CBD diameter ≥ 8 mm, pericholecystic fat infiltration, and papillitis) translated into a nomogram allows a reliable estimation of CBD stone presence. It may serve as a decision support tool to determine whether to proceed to further diagnostic tests or treatment option.

Key Points

- *CBD diameter ≥ 8 mm (odds ratio [OR] = 10.12, p < 0.001), pericholecystic fat infiltration (OR = 3.76, p = 0.014), and papillitis (OR = 2.85, p = 0.049) were independent predictors of radiolucent CBD stones.*
- *A CBD diameter ≥ 8 mm was the best predictor of CBD stones.*
- *A nomogram based on a combination of these three CT signs predicted the presence of CBD stones and helped classify patients that should go immediately to ERCP, those who require a further investigation, and those who can safely be managed conservatively.*

Keywords Common bile duct calculi · Diagnosis · Tomography, X-ray computed · Endoscopic retrograde cholangiopancreatography · Nomogram

Electronic supplementary material The online version of this article (https://doi.org/10.1007/s00330-019-06258-w) contains supplementary material, which is available to authorized users.

✉ Kyung Sook Shin
shinks@cnu.ac.kr

[1] Department of Radiology and Center for Imaging Science, Samsung Medical Center, Sungkyunkwan University School of Medicine, Seoul, Republic of Korea

[2] Department of Radiology, Chungnam National University Hospital, Chungnam National University College of Medicine, Daejeon, Republic of Korea

[3] Department of Radiology, Bucheon Hospital, Soonchunhyang University College of Medicine, Bucheon, Republic of Korea

[4] Department of Mathematics, Ajou University, Suwon, Republic of Korea

Abbreviations

ALP	Alkaline phosphatase
ALT	Alanine aminotransferase
AST	Aspartate aminotransferase
CBD	Common bile duct
CI	Confidence interval
CT	Computed tomography
ERCP	Endoscopic retrograde cholangiopancreatography
EUS	Endoscopic ultrasonography
GB	Gallbladder
GGT	Gamma-glutamyl transpeptidase
ICC	Intraclass correlation coefficients
MRCP	Magnetic resonance cholangiopancreatography
NPV	Negative predictive value
OR	Odds ratio
PACS	Picture archiving and communication system
PPV	Positive predictive value
ROC	Receiver operating characteristic
US	Ultrasound

Introduction

Common bile duct (CBD) stones are very common and usually suspected in patients with symptomatic gallbladder (GB) stones, acute cholangitis, or acute pancreatitis [1, 2]. The incidence of CBD stones is 8–20% among patients with GB stones [2, 3]. Acute cholangitis due to CBD stones may be fatal unless adequate treatment is provided promptly. The 2010 American Society of Gastrointestinal Endoscopy guidelines recommended to assign a risk of CBD stones in patients with symptomatic GB stones, in which only visualization of a CBD stone and a dilated CBD on ultrasound were imaging predictors [1]. Other imaging techniques were not included in these guidelines. Real-time ultrasound (US) has a relatively poor sensitivity (22–55%), however has a high specificity (87–90%) as these stones typically lodge distally in the intrapancreatic part of the CBD, where they may be obscured by duodenal gas [1, 4–8]. In addition, the predictive value of bile duct dilatation at US for the diagnosis of CBD stones was 71% [8].

CT is commonly a first-row examination in patients with acute abdominal pain. CT can detect CBD stones [4]. CT is more sensitive than ultrasound in the diagnosis of CBD stones [9–11] and helps in the differential diagnosis of malignant biliary obstruction and other complications, such as acute cholecystitis and acute biliary pancreatitis [12]. However, the sensitivity of CT for direct visualization of CBD stones (i.e., excluding indirect signs, such as bile duct dilatation) does not exceed 75% [13] because most hypo- or isoattenuating stones are less likely to be detected than heavily calcified stones. Therefore, in patients with high clinical suspicion of CBD stone, not detected on CT, physicians face the question of investigating further—magnetic resonance cholangiopancreatography (MRCP) or endoscopic ultrasonography (EUS)—before going to invasive endoscopic retrograde cholangiopancreatography (ERCP) or alternatively to stop all diagnostic investigations and presume prior stone passage or stricture. A better understanding of indirect CT signs of radiolucent CBD stones would greatly help the medical decision at this point.

Deciding directly for ERCP in patients with suspected CBD stones requires a high level of confidence because of the risk attached to this procedure: pancreatitis, cholangitis, bleeding, and bowel perforation [14–16]. A number of scoring and risk-stratification systems using various clinical and imaging parameters have been suggested to predict the presence of CBD stones [1–3, 17, 18]. However, to our knowledge, there is little data regarding the diagnosis of radiolucent CBD stones on CT. We performed this study to identify if indirect CT features would help recognize patients with high probability of CBD stone. We also developed a CT-based nomogram that quantifies the probability for radiolucent stones and facilitates decision-making.

Material and methods

Patients

The Institutional Review Board approved this retrospective study. The requirement for informed consent was waived. We retrospectively identified 808 patients who underwent CT followed by ERCP within 3 days for biliary disease between January 2010 and February 2018 from our institution's electronic medical record database. A computerized database at the Department of Radiology was used to find the CT images performed for an indication of clinically suspected CBD stones. A radiologist (K.S.S. who has 24 years of abdominal imaging experience) then reviewed the CT images of the patients with clinically suspected CBD stones and identified those who met the following inclusion criteria: (a) pre- and postcontrast CT performed to determine the presence of CBD stones; (b) no direct visualization of CBD stones on CT; and (c) final ERCP report available. A total of 696 patients were excluded after CT review for one of the following reasons: direct visualization of a CBD stone on CT ($n = 535$); malignancy in or involving the liver, pancreas, biliary system, and/or duodenum ($n = 125$); prior history of cholecystectomy ($n = 23$); intrahepatic duct stone ($n = 6$); prior biliary instrumentation for complicated calculous disease or other diagnoses ($n = 5$); and poor image quality ($n = 2$). Ultimately, 112 patients (63 men and 49 women, mean age 60.6 ± 15.8 [range, 25–87] years) were included in our study (Fig. 1). Of these 112 patients, 85 underwent (75.6%) contemporary MRCP. We

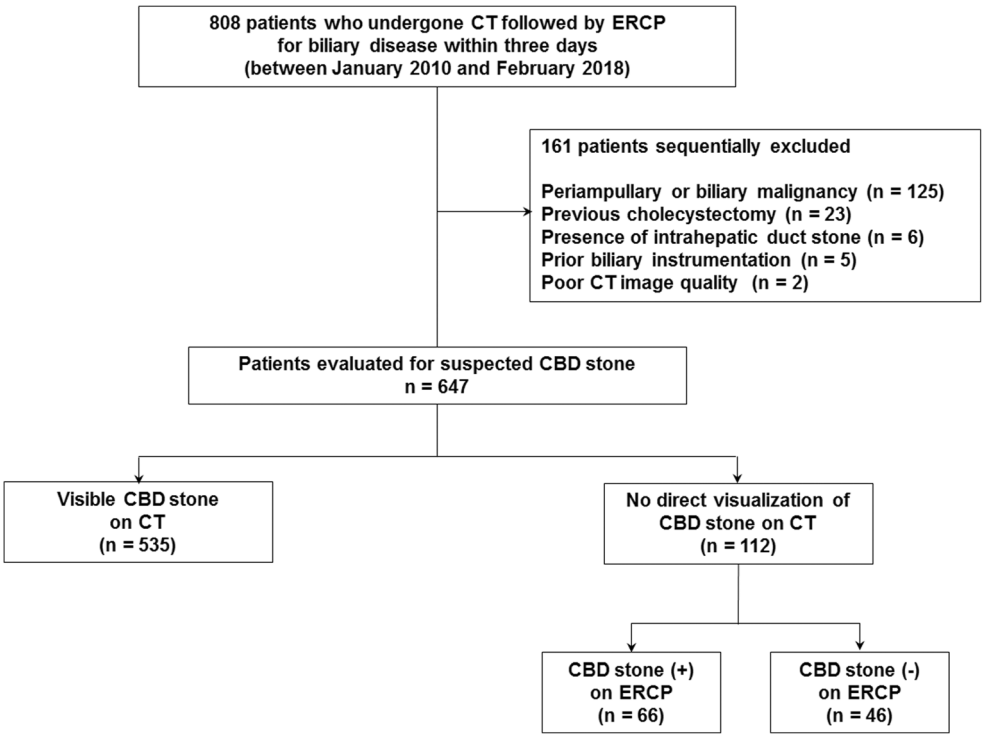

Fig. 1 Flowchart of the study population. CT, computed tomography; ERCP, endoscopic retrograde cholangiopancreatography; CBD, common bile duct

performed the subgroup analysis of these 85 patients with both CT and MRCP.

CT and MRCP technique

CT examinations were performed using multidetector CT scanners: SOMATOM Sensation 64, SOMATOM definition edge, and SOMATOM Definition Flash (all from Siemens Healthineers). CT protocols were generally determined based on the clinical impression of the physicians. The patients were asked to drink 500 mL of water to act as a neutral oral contrast just before being placed on the scanner. The scanning parameters were as follows: 100–120 kVp, 180–200 mAs, 3-mm slice thickness, table speed of 26.5–39.37 mm per rotation, and a single breath-hold helical acquisition time of 4–6 s. For contrast-enhanced CT exams, a total of 120 mL of nonionic iodinated contrast material was administered through the antecubital vein with a power injector at a rate of 3–4 mL/s. CT examinations with a dual-phase CT protocol (unenhanced and contrast-enhanced portal venous phase) or a quadruple-phase CT protocol (unenhanced and contrast-enhanced arterial, portal, and equilibrium phases) were conducted. The hepatic arterial phase scan began 30–40 s after the contrast agent injection with a bolus-tracking technique, and scanning during the portal and equilibrium phases began 65–70 s and 180 s after the start of contrast injection, respectively. Coronal and sagittal multiplanar reformation images with a 3-mm reconstruction interval were made.

The MRCP examinations were performed using a 3-T MR system (Achieva; Philips Healthcare). MR images included the following sequences: a T1-weighted turbo field-echo in-phase and opposed-phase sequence, a breath-hold multishot T2-weighted sequence, and a respiratory-triggered single-shot T2-weighted and heavily T2-weighted sequence. MRCP was performed by using two methods: a breath-hold single section two-dimensional single-shot turbo spin-echo MRCP sequence and a navigator-triggered three-dimensional MRCP turbo spin-echo sequence.

CT and MRCP image analysis

Two radiologists (J. H. M. and J. E. L, with 11 and 13 years of experience in abdominal imaging, respectively) independently reviewed all CT and MRCP images. All images were reviewed in random order on a picture archiving and communication system (PACS) (Maroview V5.4.10.42, INFINITT Healthcare). After the initial image analysis, interobserver agreement for CT features was assessed. Next, the two reviewers met to determine their final decisions by consensus for discordant cases. Neither observer was aware of the clinical or ERCP results. The reviewers assessed the following CT features: (a) CBD diameter (maximal diameter of the suprapancreatic CBD at the porta hepatis on a coronal image [13]), (b) CBD hyperenhancement (bile duct wall enhancement greater

than that of the adjacent pancreatic parenchyma during the portal venous phase [19]), (c) intrahepatic bile duct dilatation (diameter > 2 mm at the hilar duct), (d) GB luminal distension (maximum width > 4 cm and maximum length > 10 cm) [20], (e) GB wall thickening (> 3 mm) [20], (f) pericholecystic fat infiltration, (g) pericholecystic fluid collection, (h) GB stone, (i) GB sludge (increased bile attenuation within the GB [> 20 Hounsfield unit on an unenhanced scan]) [20, 21], (j) presence of pneumobilia, (k) pancreatic swelling with or without peripancreatic fat infiltration, and (l) presence of papillitis (indicated by a bulging contour with target-like or layered enhancement visible at the expected location of the duodenal papilla [22, 23]).

On MRCP, the stone is identified as a round or ovoid-shaped filling defect surrounded by the high signal intensity bile on T2WI and variable signal intensity on T1WI [24]. MRCP result was recorded as positive or negative for the diagnosis of CBD stone.

Clinical and ERCP features

The following clinical data were obtained from medical records: age, sex, reason for admission (presence of the right upper quadrant or epigastric pain, fever [> 37.4 °C], jaundice, or nausea/vomiting), and laboratory parameters. For the purposes of this study, we only assessed the first sets of laboratory parameters obtained at the time of CT acquisition.

We considered ERCP as the gold standard diagnostic method for CBD stones. When patients referred for ERCP, all clinical, biochemical, and imaging data were available to the endoscopist. It included the patient's symptom; biochemical data such as serum bilirubin, alkaline phosphatase (ALP), and/or aminotransferases; history of biliary pain or recent cholangitis or jaundice; history of recent acute pancreatitis; and suspicion of CBD stones or biliary dilatation on imaging (US, CT, MRCP, and/or EUS) before the ERCP. An ERCP diagnosis of a CBD stone was made if a stone was directly depicted at the ampulla or in the duodenum after extraction from the bile duct or if a characteristic filling defect was present within the CBD. If stones were identified, their size, number, and main composition were recorded. The size and composition were based on the largest stone. The stones were grouped by composition as follows: pigment stone (black or brown), cholesterol stone, or mixed stone. In addition, the time interval from CT or laboratory testing to therapeutic ERCP was recorded.

Statistical analysis

We used Student's *t* test or the Mann–Whitney U test for continuous variables, and the chi-square test or Fisher's exact test for categorical variables. Using receiver operating characteristic (ROC) analysis, we determined the

Table 1 Demographic data, laboratory parameters and endoscopic characteristics of patients with and without CBD stones

	ERCP findings		
	CBD stone (+) ($n = 66$)	CBD stone (−) ($n = 46$)	*p* value
Age (year)			0.036
Mean (SD)	58.2 ± 17.7	64.1 ± 11.9	
Range	25–87	31–85	
Sex			0.055
Male	32 (48.5)	31 (67.4)	
Female	34 (51.5)	15 (32.6)	
Physical examination			–
RUQ/epigastric pain	45 (68.2)	33 (71.7)	
Fever (> 37.4 °C)	9 (13.6)	7 (15.2)	
Jaundice	6 (9.1)	2 (4.3)	
Nausea/vomiting	4 (6.1)	2 (4.3)	
Laboratory test			
WBC (10^9/L)	9.7 ± 4.2	10.6 ± 5.3	0.472
CRP (mg/dL)	3.6 ± 4.5	4.6 ± 6.6	0.571
Total bilirubin (mg/dL)	3.7 ± 2.3	2.7 ± 1.5	0.009
AST (U/L)	274.7 ± 285.6	384.5 ± 413.1	0.079
ALT (U/L)	306.0 ± 301.0	253.8 ± 242.4	0.576
ALP (U/L)	187.0 ± 98.9	205.2 ± 182.9	0.640
GGT (U/L)	381.4 ± 25.0	470.8 ± 371.9	0.373
Amylase (U/L)	216.7 ± 16.0	271.5 ± 637.6	0.701
Lipase (U/L)	807.1 ± 9.0	1085.2 ± 3210.7	0.128
Stone characteristics			
Stone size (mm)*			
Mean (SD)	5.8 ± 4.1	–	
Range	1–20	–	
Stone number			
Single: multiple	42:24	–	
Stone composition †			
Pigmented stone	26 (39.4)	–	
Black stone	13 (19.7)	–	
Brown stone	13 (19.7)	–	
Cholesterol stone	32 (48.5)	–	
Mixed stone	5 (7.6)	–	

Continuous variables are described as the mean ± standard deviation, and categorical variables are described as the number of patients with the percentage in parentheses

ERCP, endoscopic retrograde cholangiopancreatography; *CBD*, common bile duct; *SD*, standard deviation; *RUQ*, right upper quadrant; *WBC*, white blood cell count; *CRP*, C-reactive protein; *AST*, aspartate aminotransferase; *ALT*, alanine aminotransferase; *ALP*, alkaline phosphatase; *GGT*, gamma-glutamyl transpeptidase

*Size is based on that of the largest stone

† Three patients failed to have stones extracted from the bile duct

Table 2 CT features of patients with and without CBD stones

	ERCP findings		κ value	p value
	CBD stone (+) ($n = 66$)	CBD stone (−) ($n = 46$)		
CBD diameter (mm), mean ± SD	10.2 ± 2.7	7.9 ± 2.8	0.82*	< 0.001
Range	5.5–19.3	4.0–16.1		
CBD subgroup†			–	< 0.001
CBD diameter ≥ 8 mm	53 (80.3)	13 (28.3)		
CBD diameter < 8 mm	13 (19.7)	33 (71.7)		
CBD hyperenhancement			0.68	0.010
Absent	17 (25.8)	23 (50.0)		
Present	49 (74.2)	23 (50.0)		
Intrahepatic duct dilatation			0.86	0.002
Absent	24 (36.4)	31 (67.4)		
Present	42 (63.6)	15 (32.6)		
GB luminal distension			0.87	0.515
Absent	51 (77.3)	33 (71.7)		
Present	15 (22.7)	13 (28.3)		
GB wall thickening			0.70	0.336
Absent	24 (36.4)	21 (45.7)		
Present	42 (63.6)	25 (54.3)		
Pericholecystic fat infiltration			0.82	0.012
Absent	28 (42.4)	31 (67.4)		
Present	38 (57.6)	15 (32.6)		
Pericholecystic fluid collection			0.85	0.243
Absent	49 (74.2)	39 (84.8)		
Present	17 (25.8)	7 (15.2)		
GB stone			0.98	0.847
Absent	35 (53.0)	26 (56.5)		
Present	31 (47.0)	20 (43.5)		
GB sludge			0.78	0.236
Absent	38 (57.6)	32 (69.6)		
Present	28 (42.4)	14 (30.4)		
Pneumobilia				0.467
Absent	60 (90.9)	44 (95.7)	1.00	
Present	6 (9.1)	2 (4.3)		
Pancreatic swelling with or without peripancreatic fat infiltration			0.82	0.441
Absent	57 (86.4)	37 (80.4)		
Present	9 (13.6)	9 (19.6)		
Papillitis			0.78	< 0.001
Absent	27 (40.9)	38 (82.6)		
Present	39 (59.1)	8 (17.4)		

Continuous variables are described as the mean ± standard deviation with a range in parentheses, and categorical variables are described as the number of patients with the percentage in parentheses

ERCP, endoscopic retrograde cholangiopancreatography; *CBD*, common bile duct; *GB*, gallbladder; *CT*, computed tomography; *CI*, confidence interval; *SD*, standard deviation

*Intraclass correlation coefficients with 95% CIs were calculated for CBD diameter

† Receiver operating characteristic analysis was used to establish the appropriate cut-off value for the CBD diameter corresponding to the maximal Youden index for discriminating two groups. This was determined as 8 mm

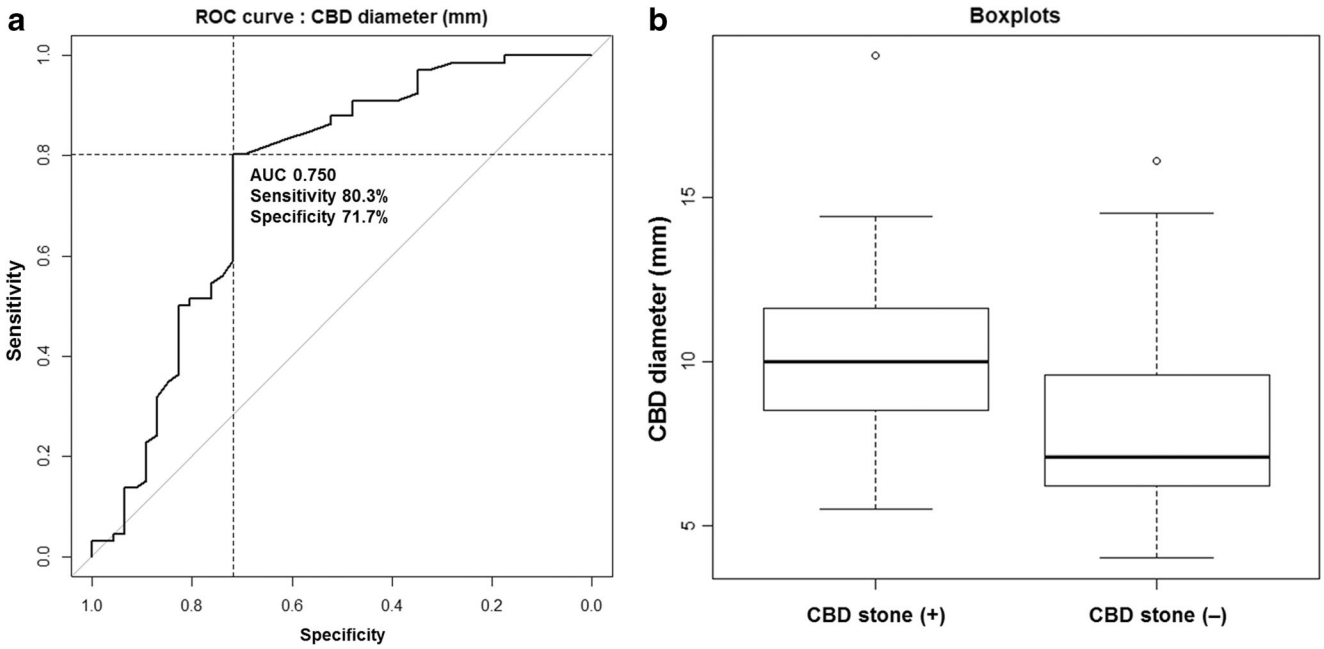

Fig. 2 CBD diameter analysis. **a** ROC curve identifying the optimal cut-off value for CBD diameter for predicting CBD stones. Cut-off value of CBD diameter is 8 mm. **b** Box-and-whisker plot of CBD diameter by presence of CBD stones. The line within each box represents the group median. The top and bottom limits of each box represent the 25th and 75th percentiles, respectively. The circles outside the boxes are outliers

Table 3 Results of the multiple logistic regression analysis for predicting CBD stones

Variables	Univariable analysis			Multivariable analysis		
	OR	95% CI	*p* value	OR	95% CI	*p* value
Age	0.98	0.95–1.00	0.053			
Male (female)	2.20	1.00–4.80	0.049			
Total bilirubin	1.29	1.04–1.60	0.019			
AST	0.99	0.99–1.00	0.116			
ALP	0.99	0.99–1.00	0.498			
GGT	0.99	0.99–1.00	0.141			
CBD diameter ≥ 8 mm (< 8 mm)	10.35	4.28–25.03	< 0.001	10.12	3.52–29.16	< 0.001
CBD hyperenhancement (absence)	2.88	1.30–6.41	0.009			
Intrahepatic duct dilatation (absence)	3.62	1.63–8.01	0.002			
GB luminal distension (absence)	0.75	0.32–1.77	0.506			
GB wall thickening (absence)	0.68	0.32–1.47	0.325			
Pericholecystic fat infiltration (absence)	2.81	1.28–6.16	0.010	3.76	1.31–10.77	0.014
Pericholecystic fluid collection (absence)	1.93	0.73–5.13	0.185			
GB stone on CT (absence)	1.15	0.54–2.46	0.715			
GB sludge on CT (absence)	1.68	0.76–3.73	0.199			
Pneumobilia (absence)	2.20	0.42–11.42	0.348			
Pancreatic swelling with or without peripancreatic fat infiltration (absence)	0.65	0.24–1.79	0.403			
Papillitis on CT (absence)	6.86	2.77–16.99	< 0.001	2.85	1.00–8.08	0.049

The reference category for each variable is presented in square brackets

CBD, common bile duct; *OR*, odds ratio; *CI*, confidence interval; *AST*, aspartate aminotransferase; *ALP*, alkaline phosphatase; *GGT*, gamma-glutamyl transpeptidase; *GB*, gallbladder

appropriate cut-off value for the CBD diameter corresponding to the maximal Youden index for discriminating two groups. To determine significant predictors of CBD stones, we used patient demographics, laboratory tests, and CT features. Multivariable logistic regression analyses were conducted with backward selection using significant variables from the univariable analysis. We calculated the sensitivity, specificity, accuracy, positive predictive value (PPV), negative predictive value (NPV), positive likelihood ratio, and negative likelihood ratio of each significant feature and combinations of these features. In addition, the predicted probability was obtained for each combination of features on the basis of the logistic regression coefficients. We compared the combination of CT features with MRCP for the diagnosis of radiolucent CBD stones.

Interobserver agreement was analyzed for each variable using kappa (k) statistics and interpreted as follows: poor, < 0.20; fair, 0.20–0.39; moderate, 0.40–0.59; substantial, 0.60–0.79; and almost perfect, 0.80–1.00. Intraclass correlation coefficients (ICC) with 95% confidence intervals (CIs) were calculated for the CBD diameter. All statistical analyses were performed using IBM SPSS Statistics for Windows, version 21.0 (IBM Corp.) and R version 3.5.0 (The R Foundation for Statistical Computing). Statistical significance was defined as a two-sided p value < 0.05.

Results

Demographic data, laboratory parameters, and ERCP characteristics

Among 647 patients with clinical suspicion of CBD stones, 112 (17.3%) had no visible CBD stones on CT. These patients were then classified by the ERCP results into a CBD stone-positive group ($n = 66$) and a CBD stone-negative group ($n = 46$) (Fig. 1). The detailed characteristics of the 112 patients are summarized in Table 1. Those in the stone-positive group were significantly younger than those in the stone-negative group (58.2 ± 17.7 years vs. 64.1 ± 11.9 years, $p = 0.036$). Jaundice was more frequently present in patients with CBD stones than in those without (9.1% [6/66] vs. 4.3% [2/46]).

Total bilirubin levels were higher in patients with CBD stones than in those without (3.7 ± 2.3 mg/dL vs. 2.7 ± 1.5 mg/dL, $p = 0.009$). There were no significant differences in the other laboratory test results.

Among 66 patients with CBD stones, 42 patients (63.6%) had a single CBD stone, and 24 (36.4%) had multiple CBD stones. The largest stone in each patient measured 5.8 ± 4.1 mm (range, 1–20); approximately half of these (48.5%, 32/66) were cholesterol stones, followed by black or brown pigment stones (both 19.7%, 13/66).

The time interval between CT and ERCP was 0–3 days (median, 1.3 days) and between laboratory testing and ERCP was 0–4 days (median, 1.7 days).

CT features

The CT features of patients are shown in Table 2. Patients with CBD stones more frequently had a larger CBD diameter ($p < 0.001$), CBD enhancement ($p = 0.015$), intrahepatic duct dilatation ($p = 0.002$), pericholecystic fat infiltration ($p = 0.016$), and papillitis ($p < 0.001$). The interobserver agreement for CT features was substantial or almost perfect ($k = 0.82$–1.00 for intrahepatic duct dilatation, GB luminal distension, pericholecystic fat infiltration, pericholecystic fluid collection, GB stones on CT, pneumobilia, and pancreatic swelling with or without peripancreatic fat infiltration; $k = 0.68$–0.80 for CBD enhancement, GB wall thickening, GB sludge on CT, and papillitis on CT). The ICC for CBD diameter across two observers was 0.82 (95% CI, 0.70–0.91) (Table 2).

The ROC curve data showed that the optimal cut-off value for CBD diameter to predict the presence of CBD stones was 8 mm, and the area under the ROC curve (AUC) was 0.750 (95% CI, 0.652–0.849). Applying this cut-off value yielded an

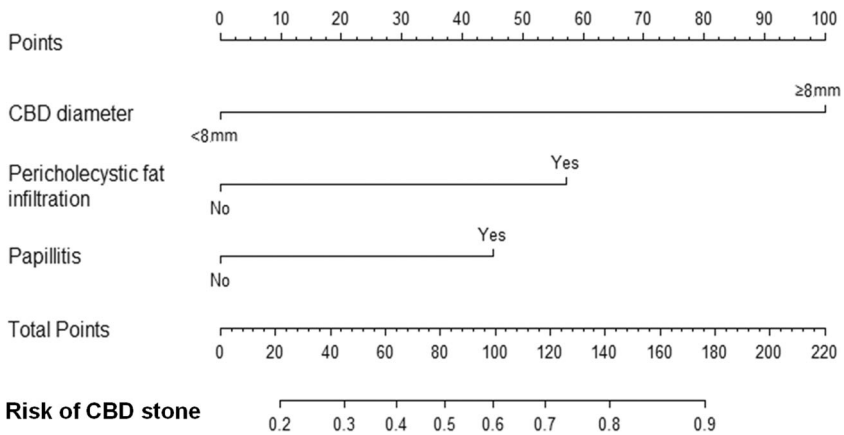

Fig. 3 CT-based nomogram for predicting CBD stones. Predictor points ("Points" scale; top) correspond to each variable. Points for all three significant CT variables are added and translated into the probability of CBD stone positivity ("Risk of CBD stone" scale; bottom)

80.3% sensitivity and a 71.7% specificity for diagnosing CBD stones (Fig. 2).

Multiple logistic regression analysis revealed that a CBD diameter ≥ 8 mm (OR = 10.12, 95% CI = 3.52–29.16, $p < 0.001$), pericholecystic fat infiltration (OR = 3.76, 95% CI = 1.31–10.77, $p = 0.014$), and papillitis (OR = 2.85, 95% CI = 1.00–8.08, $p < 0.049$) were predictors of CBD stones (Table 3). A nomogram was constructed from these significant variables (Fig. 3). Among these three significant features, a CBD diameter ≥ 8 mm showed the highest OR and was the best predictor of CBD stones using the nomogram. The diagnostic performance for these significant features, their combinations, and nomogram-calculated probability are presented in Table 4. Among them, a CBD diameter ≥ 8 mm had the highest sensitivity (80.3%, 53/66) and accuracy (76.8%, 88/112) for predicting CBD stones. In addition, papillitis had the highest specificity (82.6%, 38/46), but sensitivity was 59.1% (39/66). When two of the three features were combined, the accuracy was maintained at 75.9% (85/112), and the specificity was generally high (84.8%, 39/46). When combining any two features, incorporation of CBD diameter ≥ 8 mm tended to increase the specificity and accuracy of predicting CBD stones. When all three criteria were satisfied, the specificity was 100% (46/46) (Fig. 4). Examples of the nomogram in use are demonstrated in Fig. 4, Supplementary Fig. E1 and E2.

Comparison of CT features and MRCP

In the subgroup analysis ($n = 85$), MRCP showed better sensitivity (88.5%) and accuracy (91.9%), with 97.1% specificity for the detection of CBD stone than the combinations and nomogram-calculated probability of CT features. The comparisons of diagnostic performance between combinations of CT features and MRCP are shown in Supplementary Table E1.

Discussion

Our study demonstrated that a CBD diameter ≥ 8 mm, presence of pericholecystic fat infiltration, and papillitis on CT were significant imaging predictors of radiolucent CBD stones. Since the combination of all three features resulted in a specificity of 100%, we may safely recommend to proceed to ERCP without any further investigation in this case. This is important, as the consequences of CBD stones can be fatal, requiring an immediate treatment. Conversely, ERCP is an invasive procedure and should be avoided in patients without stones. We have introduced a CT-based nomogram that calculates the probability of the presence of radiolucent CBD stones in an individual (Fig. 3) with excellent diagnostic performance (AUC of 0.847 and accuracy of 77.7%). We expect this nomogram to contribute to a better selection of patients that are

Table 4 Diagnostic performance of three significant features and combinations for predicting CBD stones

Parameters	Total	Stone (+)	Stone (−)	Sensitivity (%)	Specificity (%)	Accuracy (%)	PPV	NPV	LR (+)	LR (−)
1. CBD diameter ≥ 8 mm	66	53	13	80.3 (53/66)	71.7 (33/46)	76.8 (88/112)	80.3 (53/66)	71.7 (33/46)	2.84 [1.77–4.57]	0.27 [0.16–0.46]
2. Pericholecystic fat infiltration	43	38	15	57.6 (38/66)	67.4 (31/46)	61.6 (69/112)	71.7 (38/53)	52.5 (31/59)	1.77 [1.11–2.81]	0.63 [0.45–0.89]
3. Papillitis on CT	47	39	8	59.1 (39/66)	82.6 (38/46)	68.8 (77/112)	83.0 (39/47)	58.5 (38/65)	3.40 [1.75–6.58]	0.50 [0.36–0.68]
1 + 2	31	31	0	47.0 (31/66)	100.0 (46/46)	68.8 (77/112)	100.0 (31/31)	56.8 (46/81)	–	0.53 [0.42–0.67]
1 + 3	39	36	3	54.6 (36/66)	93.5 (43/46)	70.5 (79/112)	92.3 (36/39)	58.9 (43/73)	8.36 [2.74–25.53]	0.49 [0.37–0.64]
2 + 3	29	25	4	38.9 (25/66)	91.3 (42/46)	59.8 (67/112)	86.2 (25/29)	50.6 (42/83)	4.36 [1.62–11.68]	0.68 [0.55–0.84]
Any two	53	46	7	69.7 (46/66)	84.8 (39/46)	75.9 (85/112)	86.8 (46/53)	66.1 (39/59)	4.58 [2.27–9.23]	0.36 [0.24–0.53]
1 + 2 + 3*	23	23	0	34.9 (23/66)	100.0 (46/46)	61.6 (69/112)	100.0 (23/23)	51.7 (46/89)	–	0.65 [0.55–0.78]
Nomogram calculated probability of CBD stone										
≥ 90% probability*	23	23	0	34.9 (23/66)	100.0 (46/46)	61.6 (69/112)	100.0 (23/23)	51.7 (46/89)	–	0.65 [0.55–0.78]
≥ 50% probability	73	55	18	83.3 (55/66)	60.9 (28/46)	74.1 (83/112)	75.3 (55/73)	71.8 (28/38)	2.13 [1.46–3.10]	0.27 [0.15–0.49]
≥ 30% probability	90	61	29	92.4 (61/66)	37.0 (17/46)	69.6 (78/112)	67.8 (61/90)	77.3 (17/22)	1.47 [1.16–1.85]	0.20 [0.08–0.52]

Data are number of patients, unless otherwise indicated; data in parentheses are numerator/denominator of patients; data in square brackets are 95% CIs

CBD, common bile duct; *CT*, computed tomography; *PPV*, positive predictive value; *NPV*, negative predictive value; *LR* (+), positive likelihood ratio; *LR* (−), negative likelihood ratio

*All three CT features have the same meaning as ≥ 90% probability on nomogram

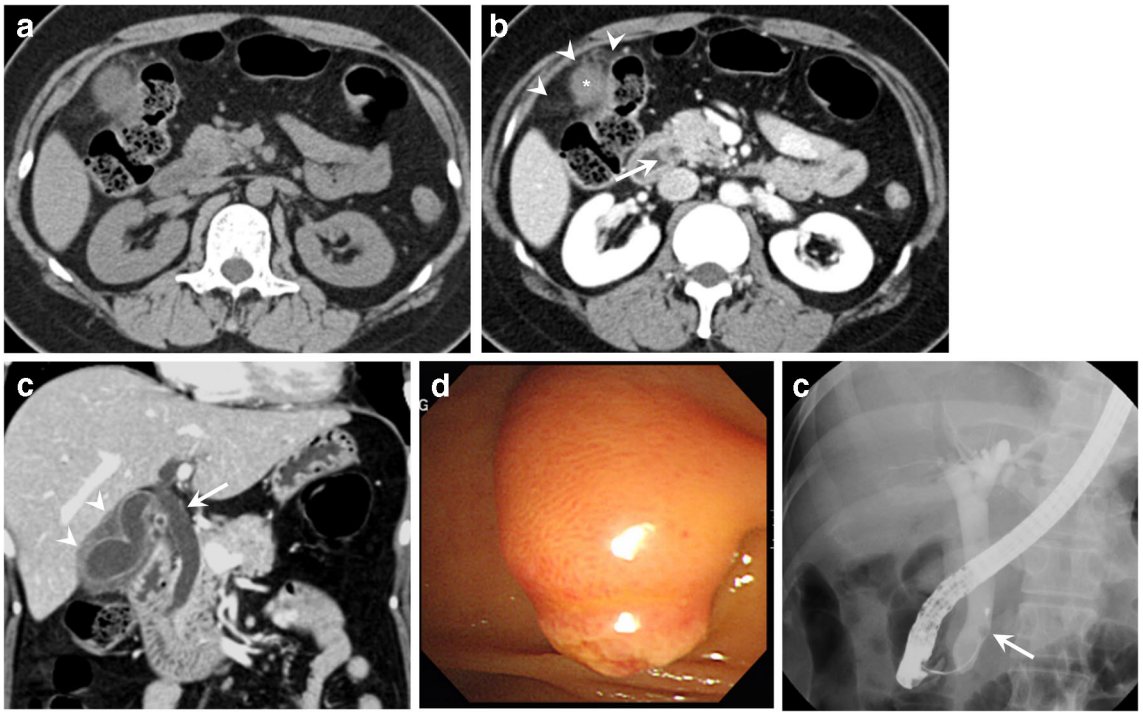

Fig. 4 A 40-year-old woman with right upper abdominal quadrant pain with radiolucent CBD stone. **a** Axial unenhanced CT scan shows no visible stone in the distal CBD. **b** Axial portal-phase CT scan obtained at the same level shows mild bulging of the papilla with increased target-like enhancement (arrow). Pericholecystic fat infiltration (arrowheads) is visible around the GB fundus (asterisk). **c** Coronal portal-phase CT scan shows a 12.2-mm maximal diameter suprapancreatic CBD at the porta hepatis (arrow). Diffuse GB wall thickening was also note (arrowheads). **d** Endoscopic image shows marked bulging of the papilla caused by the impacted stone in the ampulla of Vater. **e** Endoscopic retrograde cholangiopancreatography image confirms the presence of stone (arrow) in distal CBD. A 6-mm-size cholesterol stone was extracted. **f** The probability of CBD stone assessed by nomogram is more than 90%

candidates to ERCP, and in the other ones, if further non-invasive investigation is useful or not. The originality of our study is to incorporate CT features observed in patients without visible CBD stones on CT. Approximately 20% of CBD stones are composed purely of cholesterol [25]; in our study, cholesterol stones accounted for approximately half of all the CBD stones (48.5%, 32/66). Because these stones are isoattenuated or minimally hypoattenuated compared with surrounding bile, CT images are less sensitive for detecting them and therefore indirect CT signs become important.

A CBD diameter ≥ 8 mm was a predictor of radiolucent CBD stones. This feature was the best single predictor according to the nomogram. CBD dilation > 8 mm in a patient with an intact GB usually indicates biliary obstruction [9] and the importance of a dilated CBD as a predictor of stones is in line with the previous results [2, 26–28]. However, in previous studies, CBD measurements were mostly performed using ultrasound, not CT. CT is a very common initial investigation in patients with acute abdominal symptoms and, besides all other diseases, it is the most objective method for the rapid diagnosis of CBD stones, acute cholangitis, and identification of complications [12].

Among the three features, papillitis had the highest specificity (82.6%, 38/46) for predicting the CBD stones. CBD stones are the most common cause of acute papillitis [29]. Kim et al suggested that bulging of the papilla with increased target-like enhancement indicates an isoattenuating CBD stone [23, 29]. Bulging of the papilla may be due to edematous thickening at the ampulla of Vater, which is precipitated by mechanical irritation from a CBD stone or an impacted stone within the ampulla. In addition, an inflamed papilla usually displays homogeneously increased enhancement [23]. The finding of papillitis may also be caused by a recently passed stone or microlithiasis. However, even in this situation, drainage of infected bile via ERCP may be helpful in relieving the patient's symptoms and reducing the risk of concomitant acute cholangitis.

The third independent feature indicating radiolucent CBD stones on CT was pericholecystic fat infiltration. This is one of the major criteria for, and a fairly specific sign of, acute cholecystitis [30]. The presence of an impacted CBD stone may cause biliary obstruction and increase the viscosity of bile. As biliary obstruction progresses, acute cholecystitis can be provoked by distension of the GB. The presence of pericholecystic infiltration may be interpreted as a sign of significant biliary obstruction by a CBD stone.

Interestingly, among the various laboratory tests, only total bilirubin tends to be elevated in patients with CBD stones in univariable analysis, but not in multivariable analysis. AST, ALP, and GGT, as well as total bilirubin, are known predictors of CBD stones [2, 18], yet in the present study, the PPV of abnormal laboratory parameters was only 15–50% [1]. CBD stones that are only partially obstructive might not elevate bilirubin levels, whereas microlithiasis or sludge in the CBD can increase the viscosity of bile, causing both ALP and bilirubin levels to rise [18]. In addition, these cholestatic parameters increase progressively with the duration and severity of biliary obstruction [1]. Therefore, the time interval between blood sampling and ERCP or trend observations in laboratory tests may influence the true predictive ability of these parameters.

Compared with MRCP, the combination of CT features and nomogram showed lower diagnostic performance for the presence of CBD stone, as expected. However, they can be used as a clinical decision support tool. Based on the results of this study, we may propose the following approach. Patients with all three CT features (≥ 90% probability on nomogram) may proceed to ERCP without additional imaging tests. This direct and quick approach is important because ERCP should not be delayed in patients with acute cholangitis due to CBD stone [31, 32]. In patients with at least one of three CT features (≥ 30% probability of nomogram), EUS or MRCP may be recommended before deciding whether ERCP is needed. Finally, patients without any of the three CT features can be managed conservatively.

Our study has several limitations. First, it was inherently limited by the retrospective single-center design with a probable selection bias. Because our study included patients who finally underwent ERCP, it may result in a positive bias in the reported statistics. Second, subjective criteria were used to evaluate CT signs; nevertheless, these criteria are used in clinical practice, and despite their subjective nature, the interobserver agreement for each was substantial to perfect in our study. Third, we decided to exclude patients who underwent cholecystectomy to generate a homogeneous cohort because of the relationship between cholecystectomy and the diameter of the CBD. Fourth, we cannot exclude the possibility of passage of CBD stones during the time interval between CT examination and ERCP. Fifth, using CT for initial evaluation of CBD stone in the emergency setting may not be the standard practice in all institutions. Last, we did not perform an external analysis using an independent validation set to determine thresholds for the ratios used to construct the nomogram; therefore, these values need to be validated through a larger, prospective study.

In conclusion, we have shown that a combination of three CT features (CBD diameter ≥ 8 mm, pericholecystic fat infiltration, and papillitis) and CT-based nomogram would allow estimating the probability of radiolucent CBD stones. It may serve as a decision support tool to determine whether to proceed to further diagnostic tests or treatment option.

Funding The authors state that this work has not received any funding.

Compliance with ethical standards

Guarantor The scientific guarantor of this publication is Kyung Sook Shin in the Department of Radiology, Chungnam National University Hospital, Chungnam National University College of Medicine, Daejeon, Republic of Korea.

Conflict of interest The authors of this manuscript declare no relationships with any companies whose products or services may be related to the subject matter of the article.

Statistics and biometry Two of the authors have significant statistical expertise (Seo-Youn Choi and Soohyun Ahn).

Informed consent Written informed consent was waived by the Institutional Review Board.

Ethical approval Institutional Review Board approval was obtained.

Methodology
- Retrospective
- Observational
- Performed at one institution

References

1. Maple JT, Ben-Menachem T, Anderson MA et al (2010) The role of endoscopy in the evaluation of suspected choledocholithiasis. Gastrointest Endosc 71:1–9
2. Kamath SU, Dharap SB, Kumar V (2016) Scoring system to preoperatively predict choledocholithiasis. Indian J Gastroenterol 35: 173–178
3. Tozatti J, Mello AL, Frazon O (2015) Predictor factors for choledocholithiasis. Arq Bras Cir Dig 28:109–112
4. Jeffrey RB, Federle MP, Laing FC, Wall S, Rego J, Moss AA (1983) Computed tomography of choledocholithiasis. AJR Am J Roentgenol 140:1179–1183
5. Einstein DM, Lapin SA, Ralls PW, Halls JM (1984) The insensitivity of sonography in the detection of choledocholithiasis. AJR Am J Roentgenol 142:725–728
6. Cronan JJ (1986) US diagnosis of choledocholithiasis: a reappraisal. Radiology 161:133–134
7. Gross BH, Harter LP, Gore RM et al (1983) Ultrasonic evaluation of common bile duct stones: prospective comparison with endoscopic retrograde cholangiopancreatography. Radiology 146:471–474
8. O'Connor HJ, Hamilton I, Ellis WR, Watters J, Lintott DJ, Axon AT (1986) Ultrasound detection of choledocholithiasis: prospective comparison with ERCP in the postcholecystectomy patient. Gastrointest Radiol 11:161–164
9. Baron RL, Stanley RJ, Lee JK et al (1982) A prospective comparison of the evaluation of biliary obstruction using computed tomography and ultrasonography. Radiology 145:91–98

10. Pasanen P, Partanen K, Pikkarainen P, Alhava E, Pirinen A, Janatuinen E (1992) Ultrasonography, CT, and ERCP in the diagnosis of choledochal stones. Acta Radiol 33:53–56
11. Mitchell SE, Clark RA (1984) A comparison of computed tomography and sonography in choledocholithiasis. AJR Am J Roentgenol 142:729–733
12. Kiriyama S, Takada T, Strasberg SM et al (2013) TG13 guidelines for diagnosis and severity grading of acute cholangitis (with videos). J Hepatobiliary Pancreat Sci 20:24–34
13. Neitlich JD, Topazian M, Smith RC, Gupta A, Burrell MI, Rosenfield AT (1997) Detection of choledocholithiasis: comparison of unenhanced helical CT and endoscopic retrograde cholangiopancreatography. Radiology 203:753–757
14. Freeman ML (2012) Complications of endoscopic retrograde cholangiopancreatography: avoidance and management. Gastrointest Endosc Clin N Am 22:567–586
15. Loperfido S, Angelini G, Benedetti G et al (1998) Major early complications from diagnostic and therapeutic ERCP: a prospective multicenter study. Gastrointest Endosc 48:1–10
16. Freeman ML (2002) Adverse outcomes of endoscopic retrograde cholangiopancreatography. Rev Gastroenterol Disord 2:147–168
17. Al-Jiffry BO, Khayat S, Abdeen E, Hussain T, Yassin M (2016) A scoring system for the prediction of choledocholithiasis: a prospective cohort study. Ann Saudi Med 36:57–63
18. Videhult P, Sandblom G, Rudberg C, Rasmussen IC (2011) Are liver function tests, pancreatitis and cholecystitis predictors of common bile duct stones? Results of a prospective, population-based, cohort study of 1171 patients undergoing cholecystectomy. HPB (Oxford) 13:519–527
19. Kim SW, Kim SH, Lee DH et al (2017) Isolated Main pancreatic duct dilatation: CT differentiation between benign and malignant causes. AJR Am J Roentgenol 209:1046–1055
20. Choi SY, Lee HK, Yi BH et al (2018) Pope's hat sign: another valuable CT finding of early acute cholecystitis. Abdom Radiol (NY) 43:1693-1702
21. Kim YK, Kwak HS, Kim CS et al (2009) CT findings of mild forms or early manifestations of acute cholecystitis. Clin Imaging 33:274–280
22. Jang KM, Kim SH, Lee SJ, Park HJ, Choi D, Hwang J (2013) Added value of diffusion-weighted MR imaging in the diagnosis of ampullary carcinoma. Radiology 266:491–501
23. Kim S, Lee NK, Lee JW et al (2007) CT evaluation of the bulging papilla with endoscopic correlation. Radiographics 27:1023–1038
24. Lee NK, Kim S, Lee JW et al (2010) MR appearance of normal and abnormal bile: correlation with imaging and endoscopic finding. Eur J Radiol 76:211–221
25. Ajlan AM, Mesurolle B, Stein L et al (2015) Detectability of choledocholithiasis on CT: the effect of positive intraduodenal enteric contrast on portovenous contrast-enhanced studies. Saudi J Gastroenterol 21:306–312
26. Prat F, Meduri B, Ducot B, Chiche R, Salimbeni-Bartolini R, Pelletier G (1999) Prediction of common bile duct stones by noninvasive tests. Ann Surg 229:362–368
27. Sgourakis G, Dedemadi G, Stamatelopoulos A, Leandros E, Voros D, Karaliotas K (2005) Predictors of common bile duct lithiasis in laparoscopic era. World J Gastroenterol 11:3267–3272
28. Miller FH, Hwang CM, Gabriel H, Goodhartz LA, Omar AJ, Parsons WG 3rd (2003) Contrast-enhanced helical CT of choledocholithiasis. AJR Am J Roentgenol 181:125–130
29. Kim TU, Kim S, Lee JW et al (2008) Ampulla of Vater: comprehensive anatomy, MR imaging of pathologic conditions, and correlation with endoscopy. Eur J Radiol 66:48–64
30. Paulson EK (2000) Acute cholecystitis: CT findings. Semin Ultrasound CT MR 21:56–63
31. Parikh MP, Gupta NM, Thota PN, Lopez R, Sanaka MR (2018) Temporal trends in utilization and outcomes of endoscopic retrograde cholangiopancreatography in acute cholangitis due to choledocholithiasis from 1998 to 2012. Surg Endosc 32:1740–1748
32. Parikh MP, Wadhwa V, Thota PN, Lopez R, Sanaka MR (2018) Outcomes associated with timing of ERCP in acute cholangitis secondary to choledocholithiasis. J Clin Gastroenterol 52:e97–e102